nature geoscience

SUPPLEMENTARY INFORMATION

DOI: 10.1038/NGEO1185

Deep-sea mud in the Pacific Ocean as a potential resource for rare-earth elements

Yasuhiro Kato[1]*, Koichiro Fujinaga[1], Kentaro Nakamura[2], Yutaro Takaya[1], Kenichi Kitamura[1], Junichiro Ohta[1], Ryuichi Toda[1], Takuya Nakashima[1] & Hikaru Iwamori[3]

[1] Department of Systems Innovation, The University of Tokyo, 7-3-1 Hongo, Bunkyo-ku, Tokyo 113-8656, Japan

[2] Precambrian Ecosystem Laboratory (PEL), Japan Agency for Marine-Earth Science and Technology (JAMSTEC), 2-15 Natsushima, Yokosuka, Kanagawa 237-0061, Japan

[3] Department of Earth and Planetary Sciences, Tokyo Institute of Technology, 2-12-1 Ookayama, Meguro-ku, Tokyo 152-8551, Japan

*e-mail: ykato@sys.t.u-tokyo.ac.jp

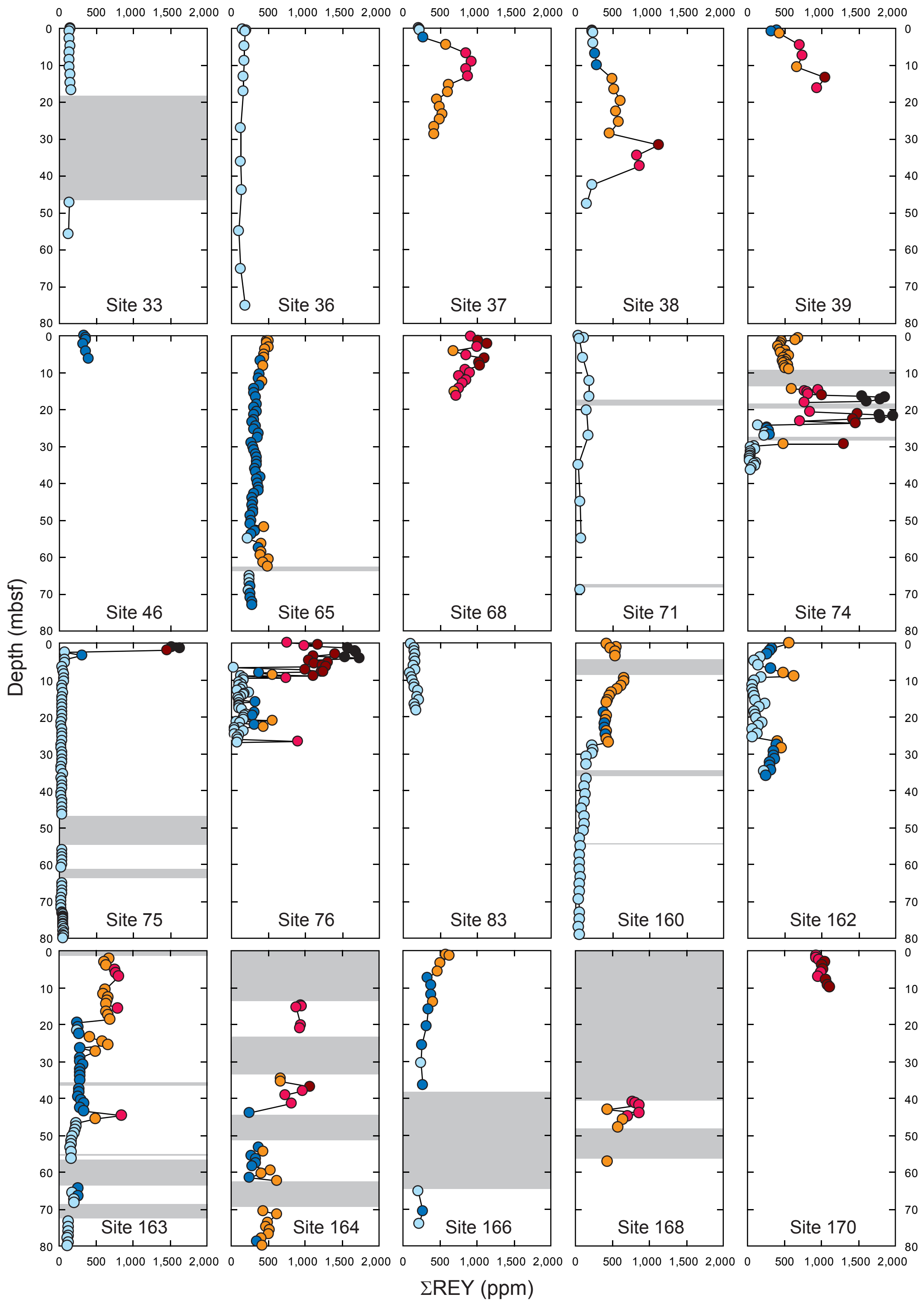

Supplementary Figure S1. Detailed depth profiles of ΣREY contents for all study cores. The pale grey intervals represent no core recovery.

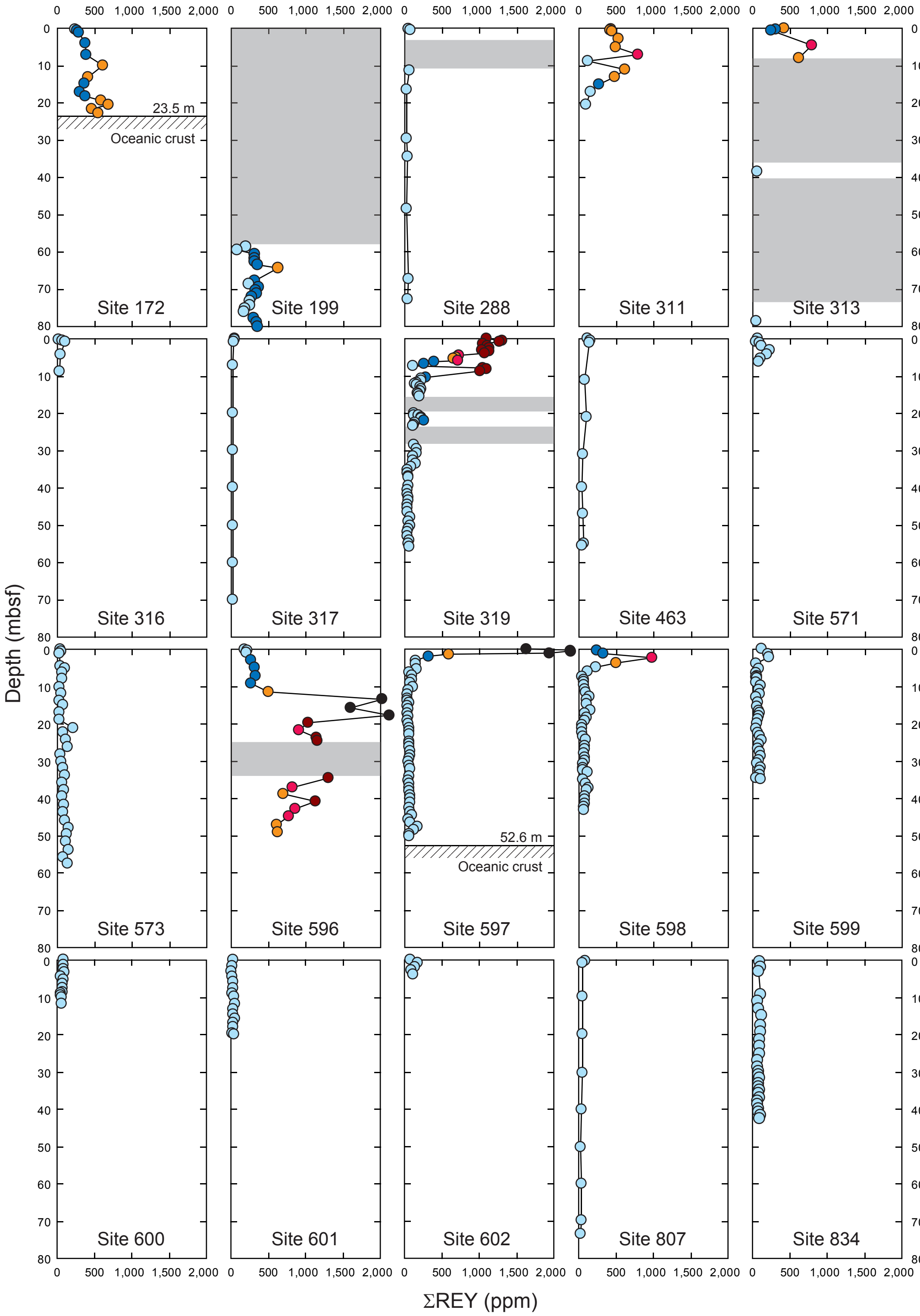

Supplementary Figure S1. *(continued.)*

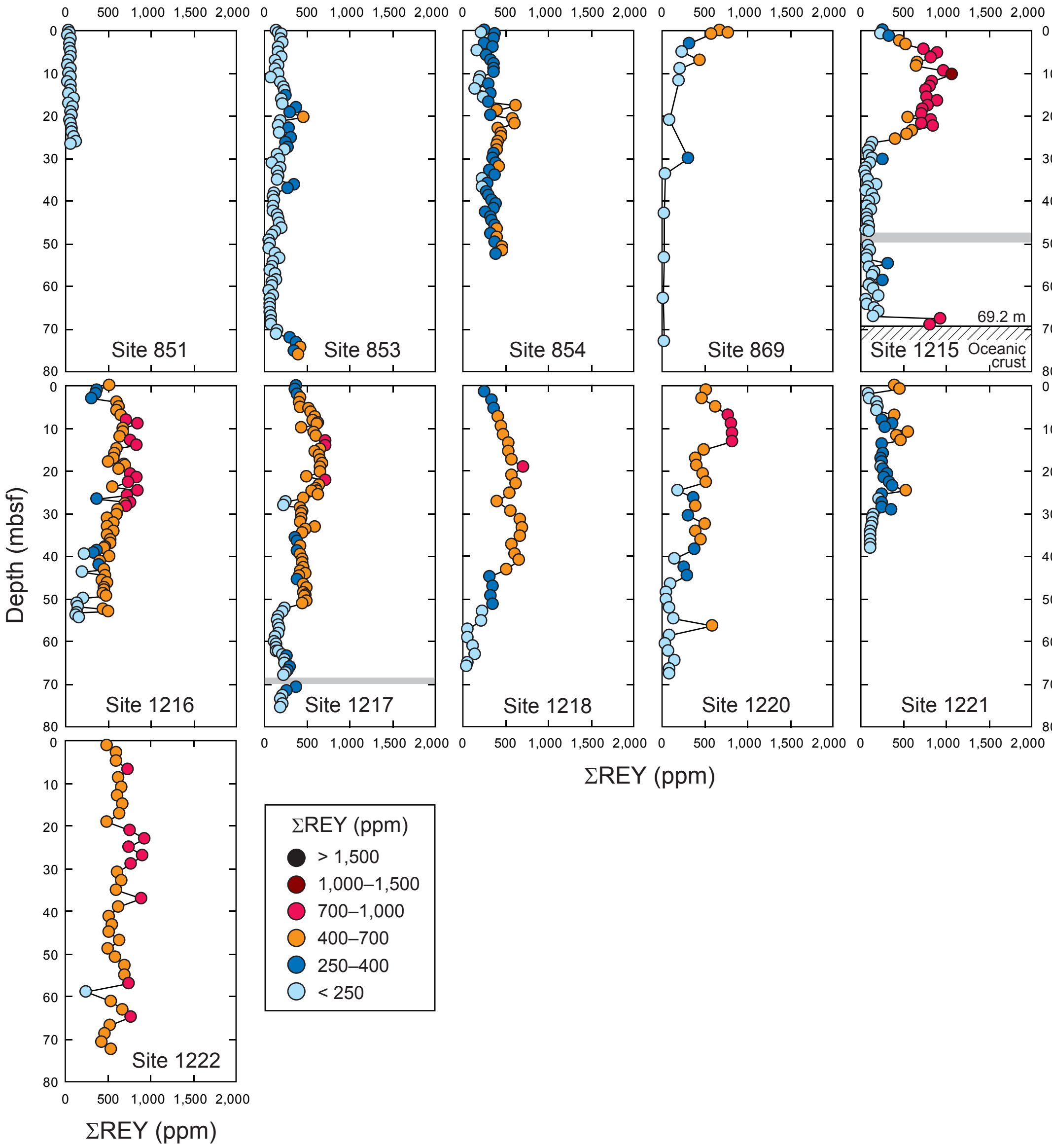

Supplementary Figure S1. *(continued.)*

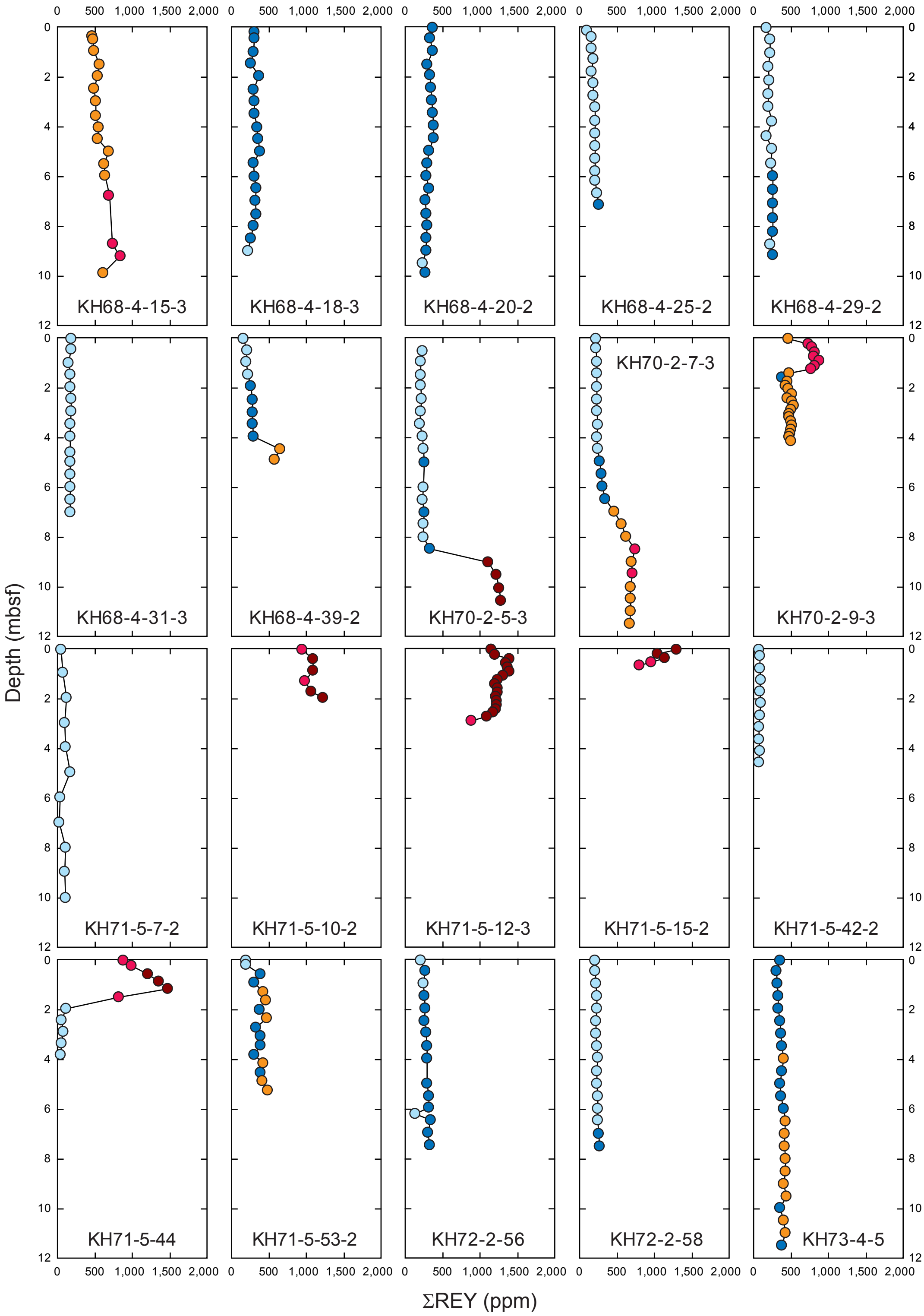

Supplementary Figure S1. *(continued.)*

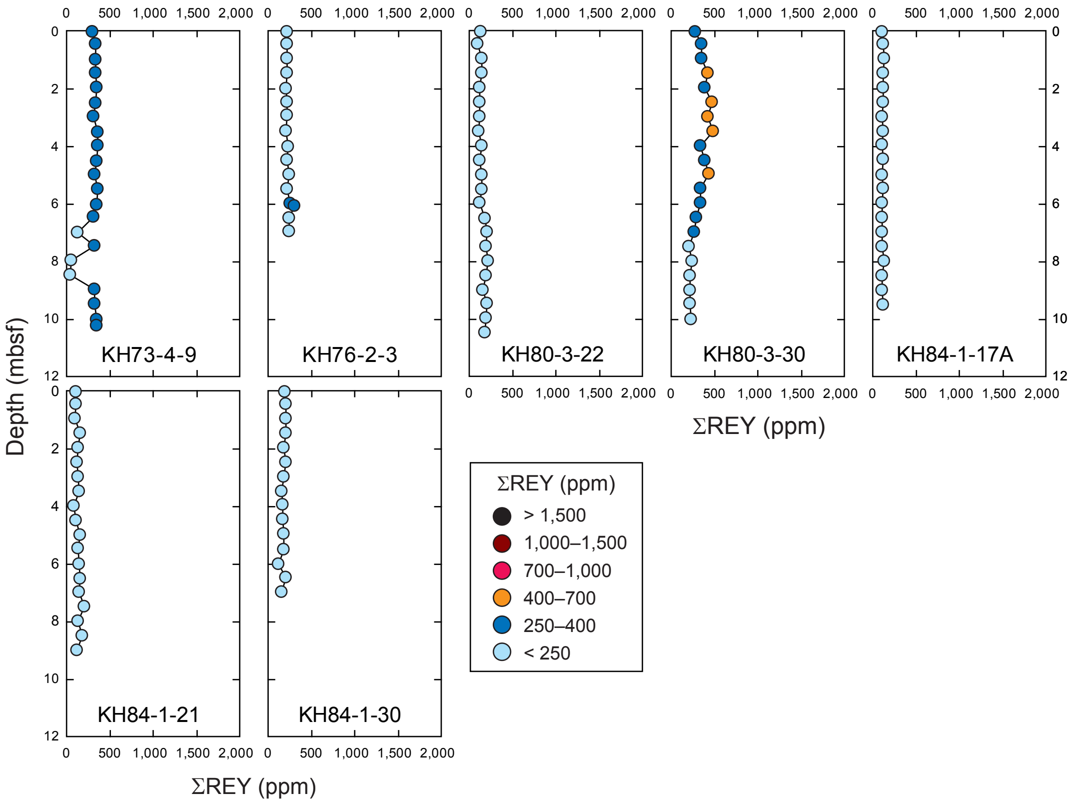

Supplementary Figure S1. *(continued.)*

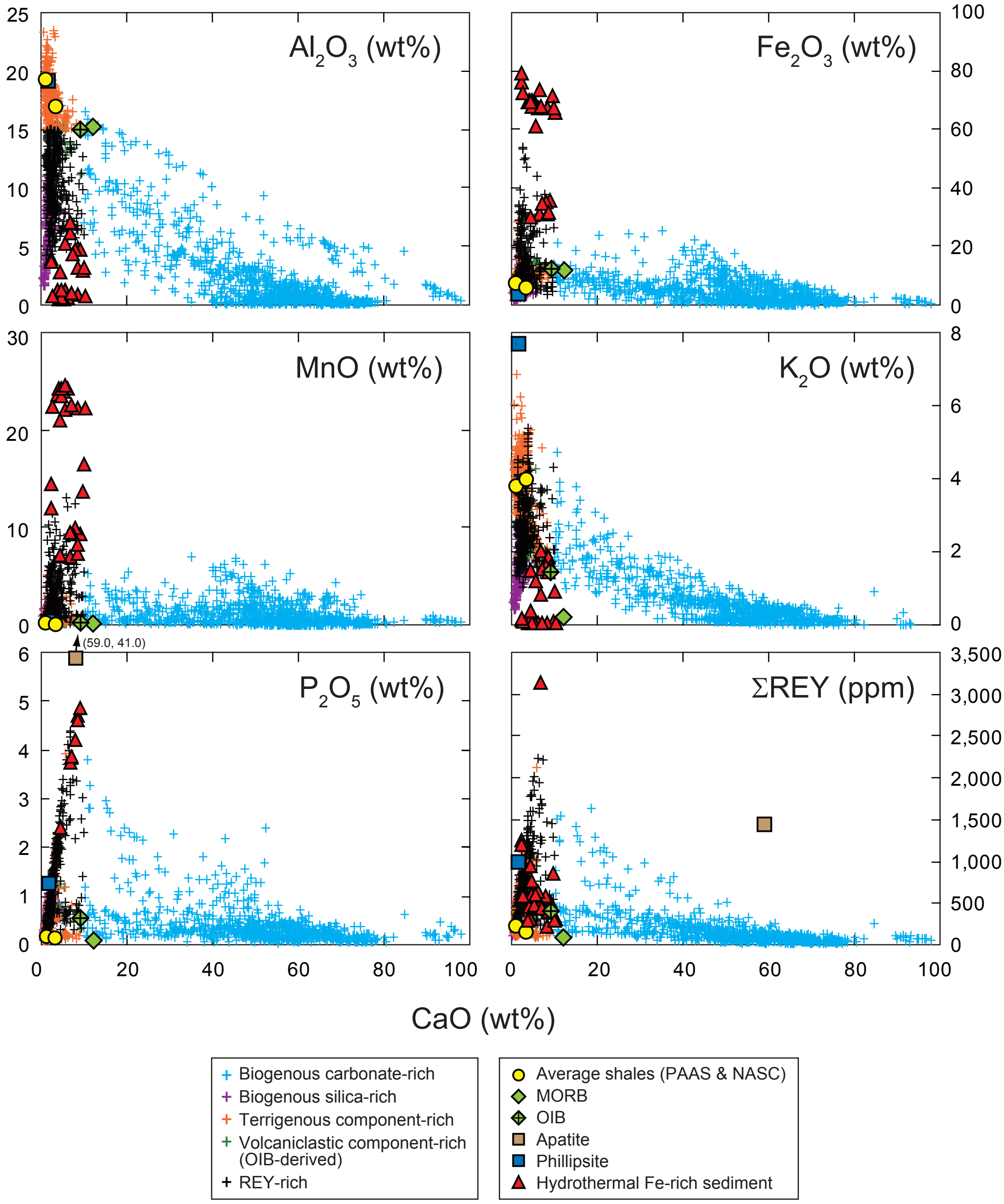

Supplementary Figure S2. CaO versus other oxides and ΣREY. To make constituent components of seafloor sediments more visible, sediments with specific compositions are colour-coded: biogenous carbonate-rich (CaO > 10 wt%) in blue, biogenous silica-rich (SiO_2 > 70 wt%) in purple, terrigenous component-rich (Al_2O_3 > 15 wt%) in orange and volcaniclastic component-rich (OIB-derived; $TiO_2 > (Al_2O_3+5)/20$) in green. The remaining samples, as shown in black, can be regarded as enriched in the REY-rich component. Major element oxide data are recalculated on a loss on ignition-free basis. The major element oxide data point of phillipsite is represented by the average content of the data by refs S1 and S2. The ΣREY content of phillipsite is given as 1,000 ppm based on the data by ref. S3. Note that two-third of the samples of hydrothermal Fe-rich sediments lack SiO_2, TiO_2 and P_2O_5 data, and have been recalculated on a carbonate-free basis. Data on endmembers: average shales (refs S4–6), MORB (ref. S7), OIB (ref. S8), apatite (ref. S9), phillipsite (refs S1–3) and hydrothermal Fe-rich sediment near mid-ocean ridge (refs S10–12).

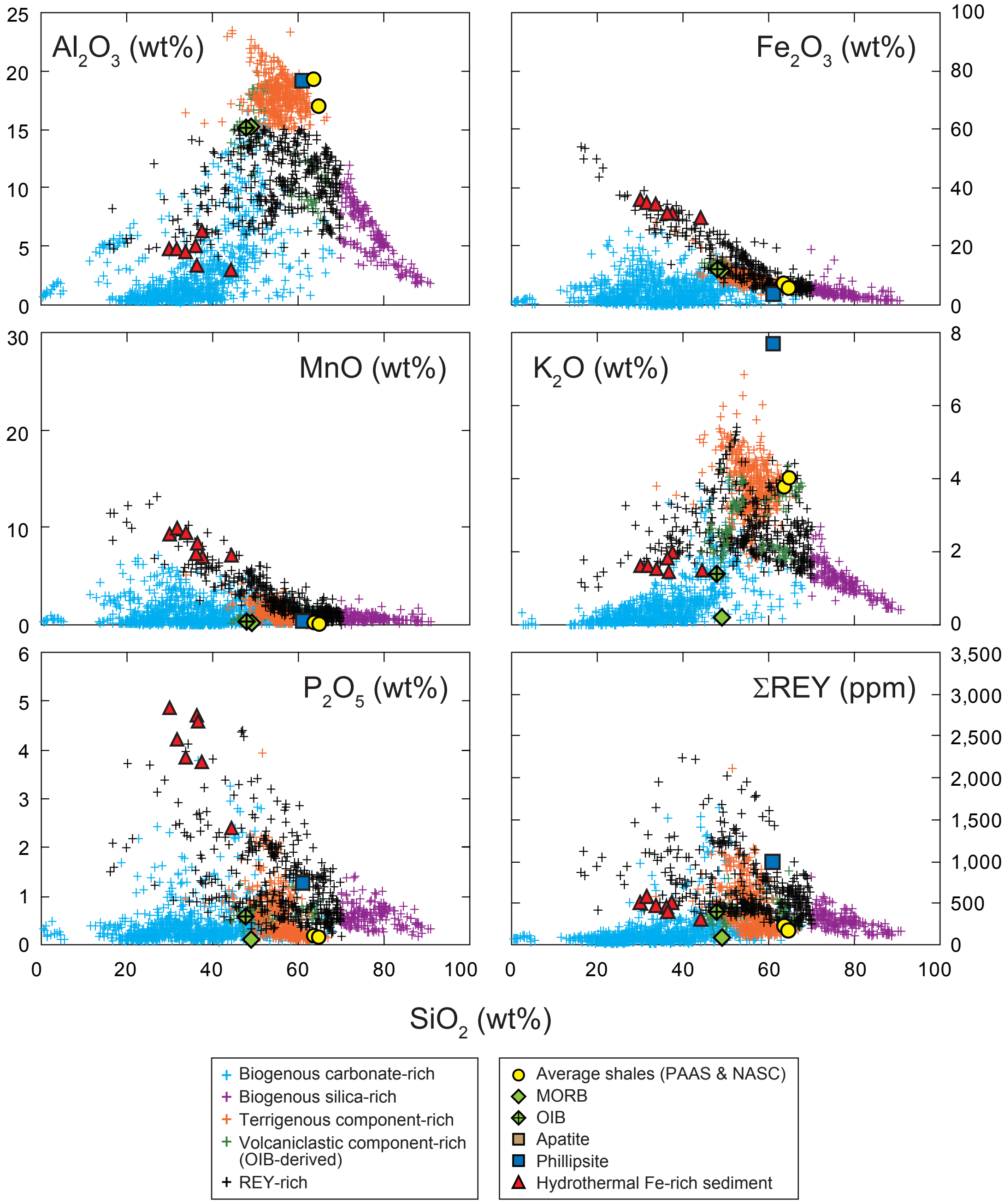

Supplementary Figure S3. SiO_2 versus other oxides and ΣREY. Symbols and the colour-coding are the same as in Supplementary Fig. S2.

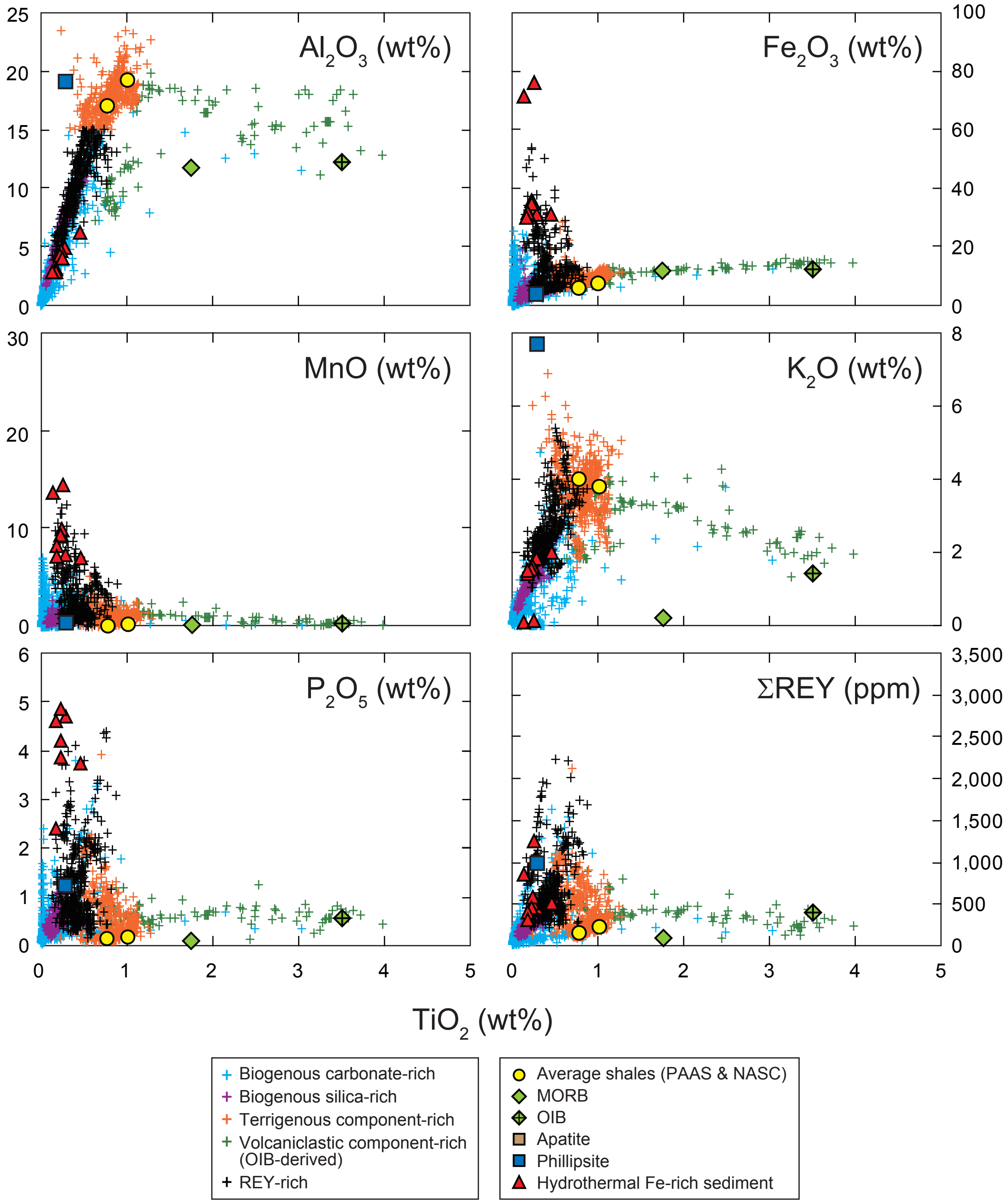

Supplementary Figure S4. TiO_2 versus other oxides and ΣREY. Symbols and the colour-coding are the same as in Supplementary Fig. S2.

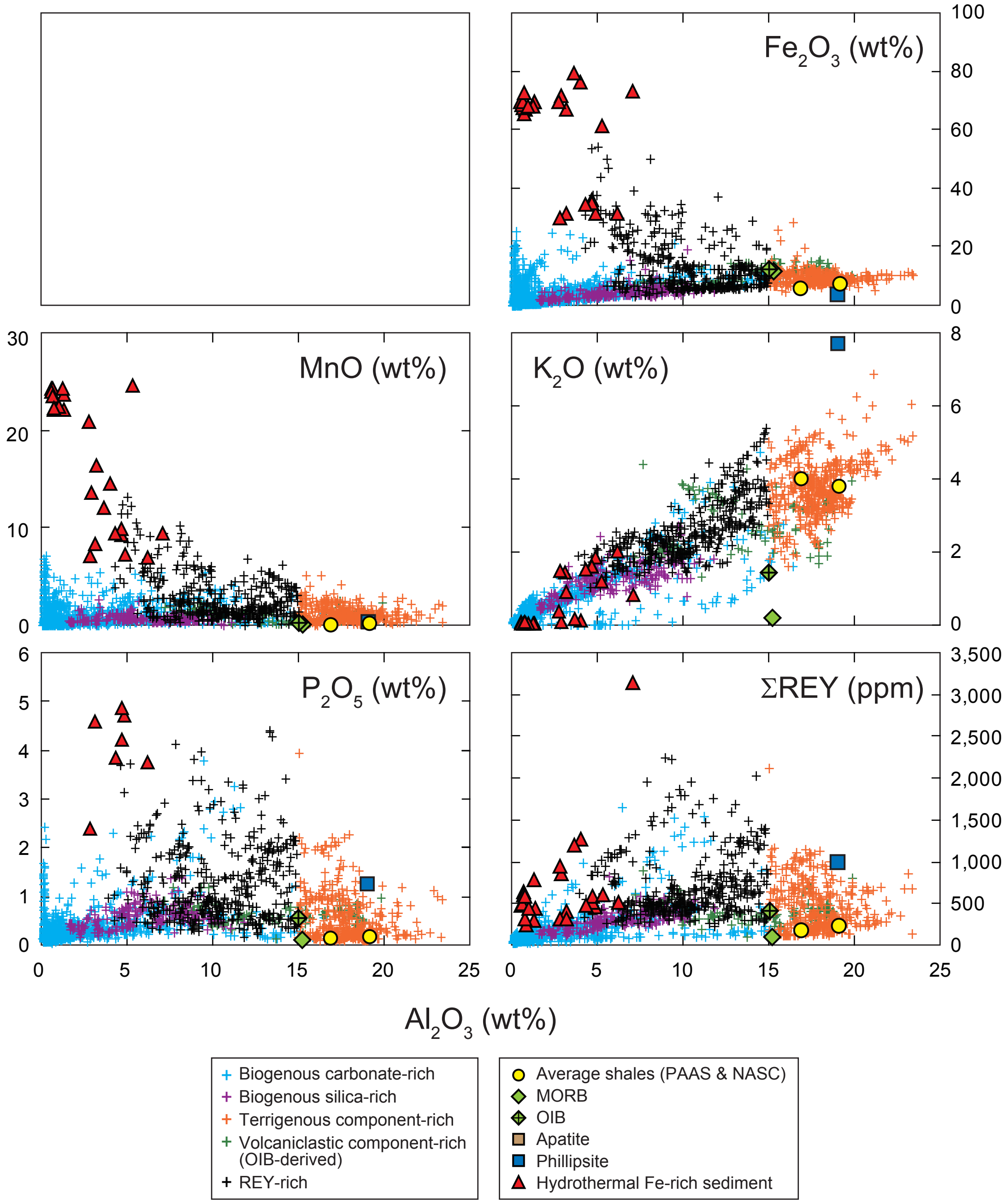

Supplementary Figure S5. Al$_2$O$_3$ versus other oxides and ΣREY. Symbols and the colour-coding are the same as in Supplementary Fig. S2.

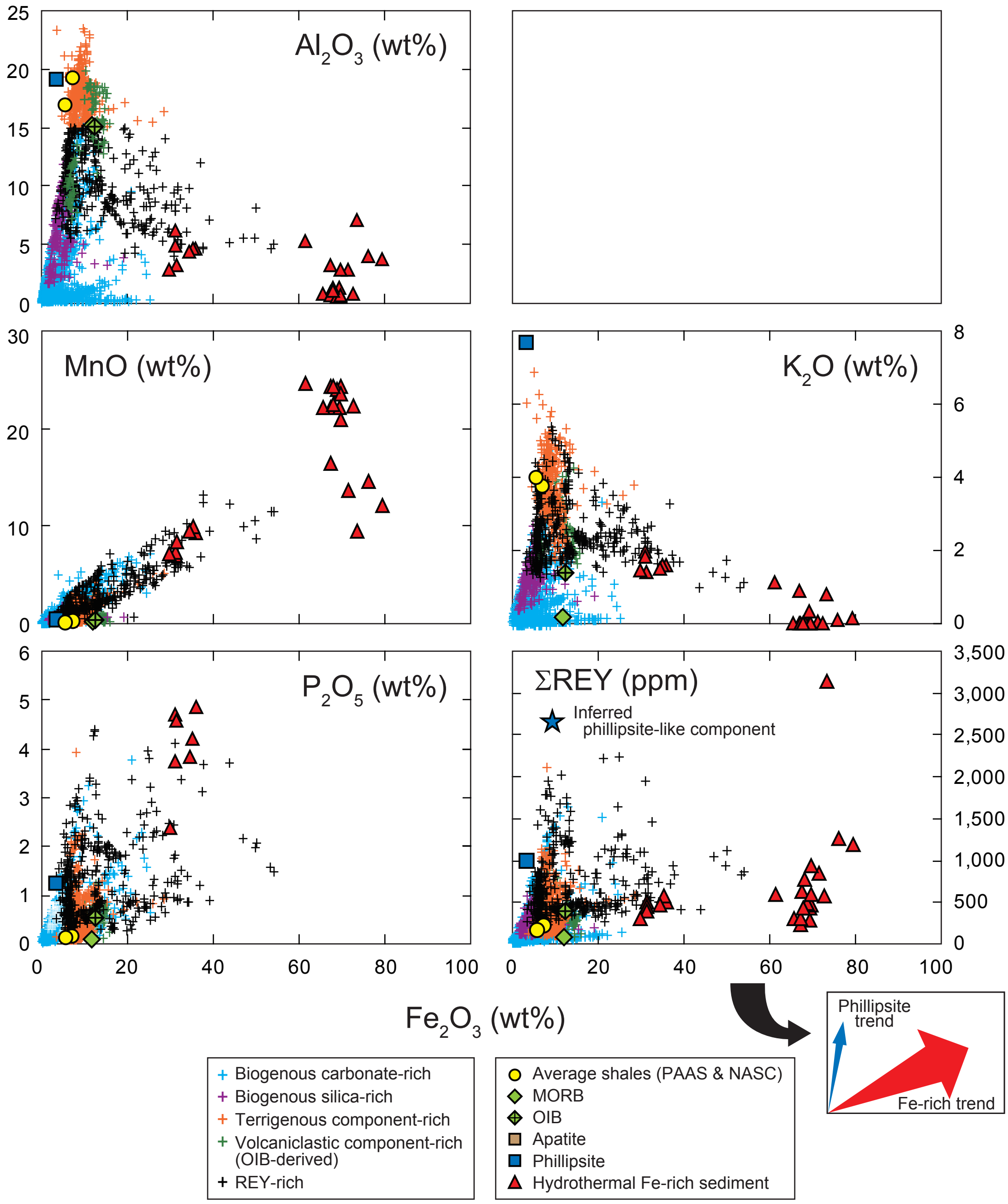

Supplementary Figure S6. Fe_2O_3 versus other oxides and ΣREY. Symbols and the colour-coding are the same as in Supplementary Fig. S2.

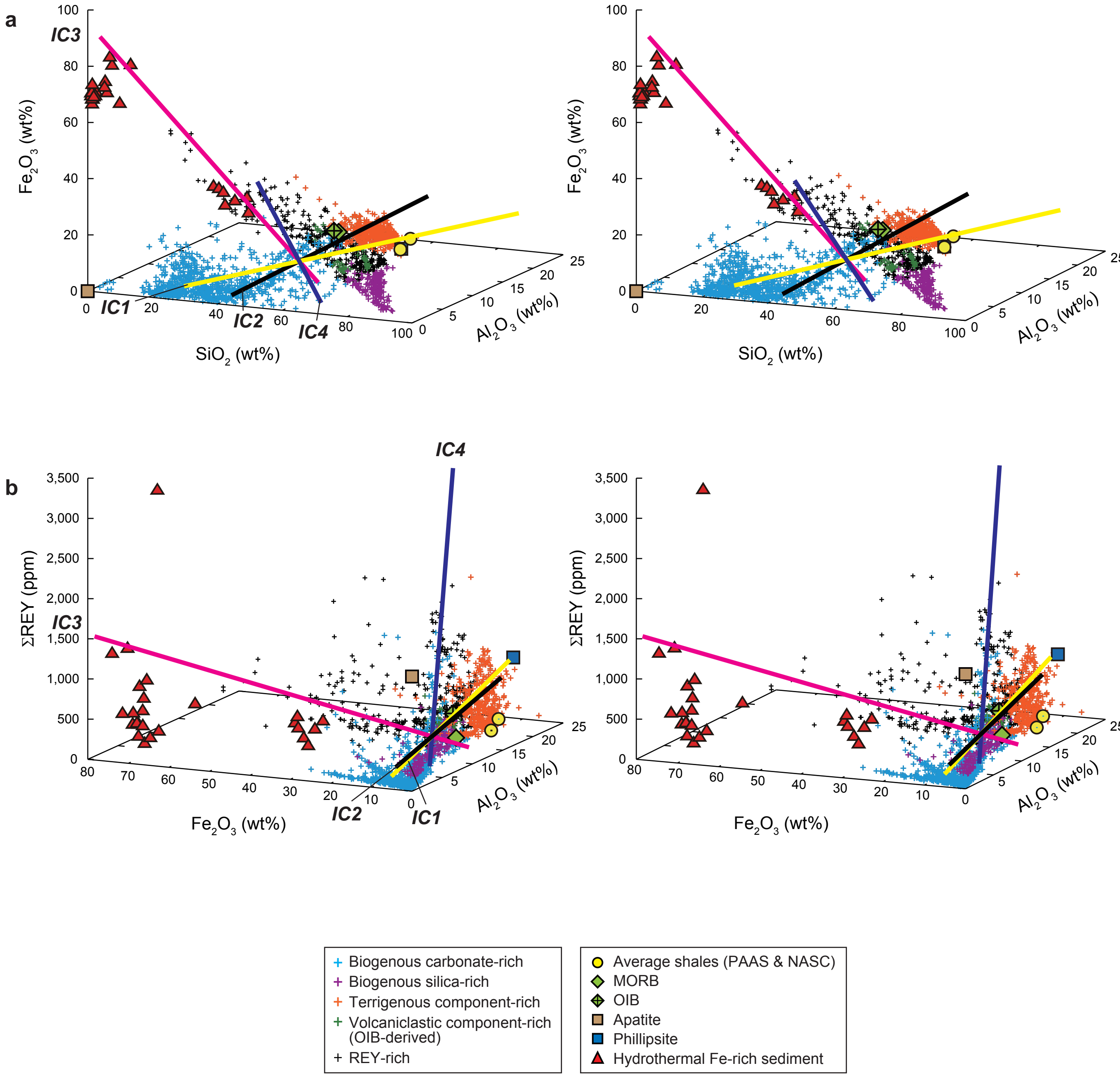

Supplementary Figure S7. Independent components (IC1 to IC4) in three-dimensional stereo plots. a, SiO_2–Al_2O_3–Fe_2O_3. **b**, Fe_2O_3–Al_2O_3–ΣREY. Independent components have been obtained with the same procedure as described in ref. S13. Symbols and the colour-coding are the same as in Supplementary Fig. S2.

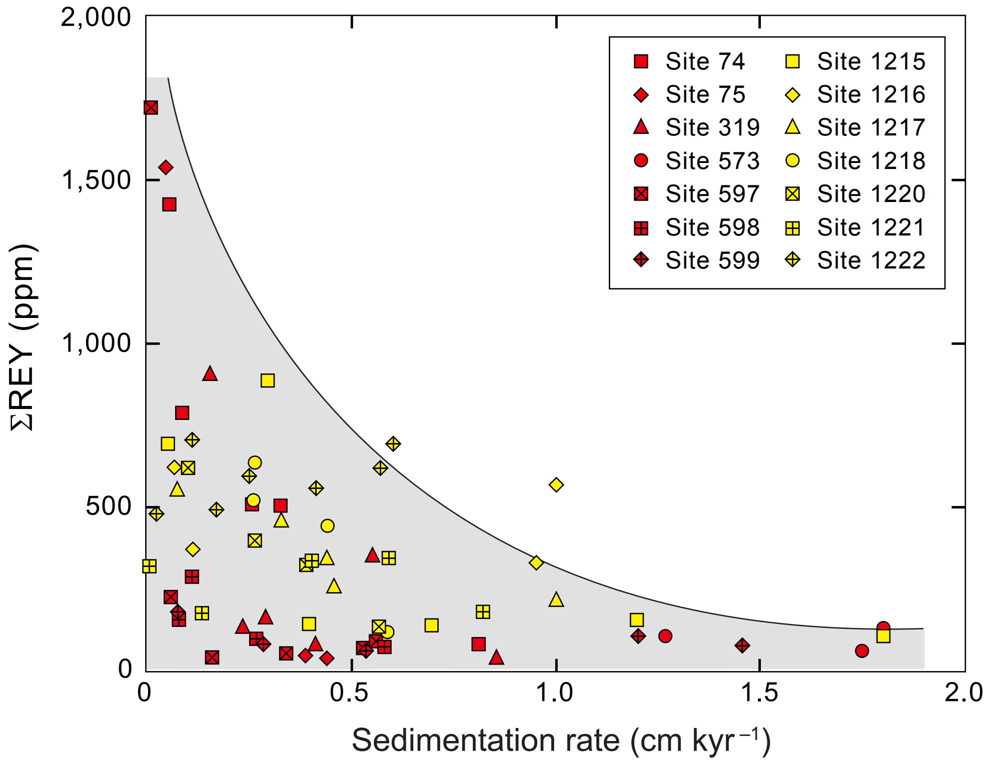

Supplementary Figure S8. Sedimentation rates versus ΣREY contents for the DSDP/ODP cores. Data on sedimentation rates are from the respective Initial Reports of the Deep Sea Drilling Project and Proceedings of the Ocean Drilling Program volumes.

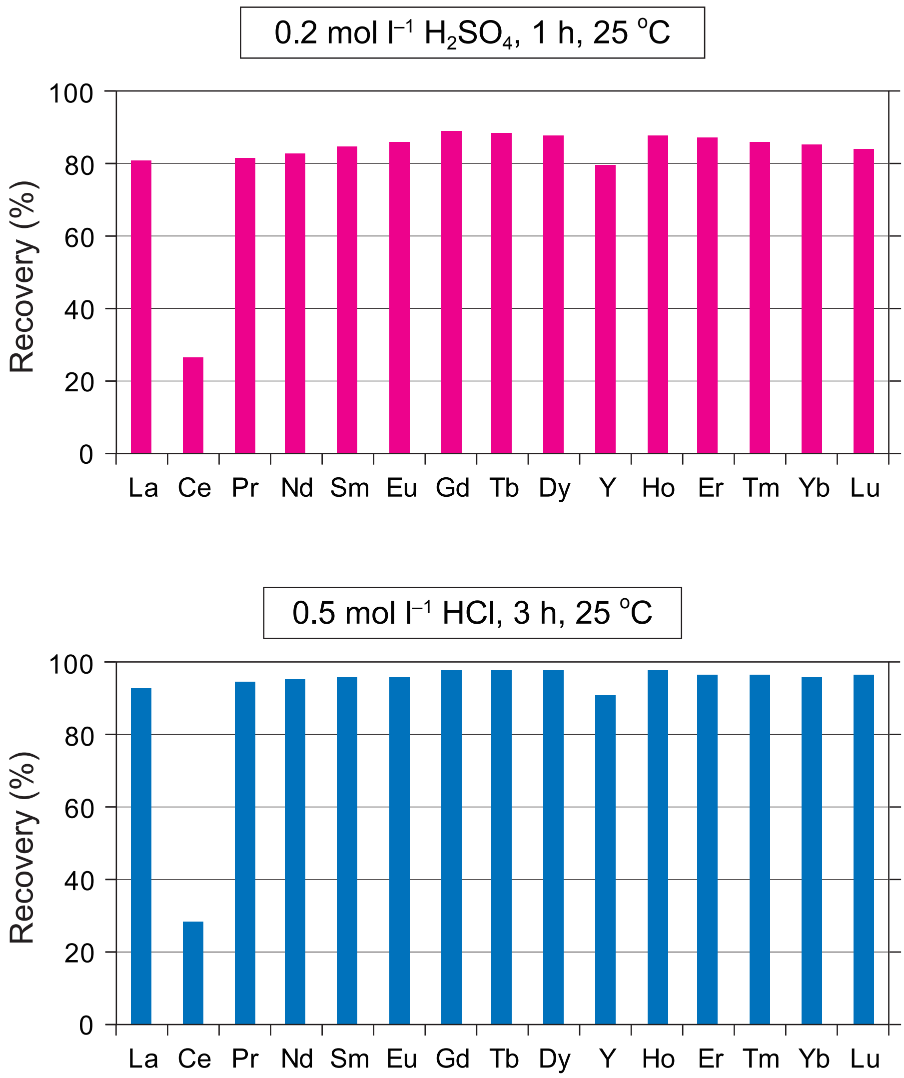

Supplementary Figure S9. Results of leaching experiments of REY from the REY-rich mud (Sample No. Site 68*, 1-2, 50-52 cm) by dilute acids. Experimental conditions are 0.2 moll^{-1} H_2SO_4, 1 h and 25°C (above) and 0.5 moll^{-1} HCl, 3 h and 25°C (below).

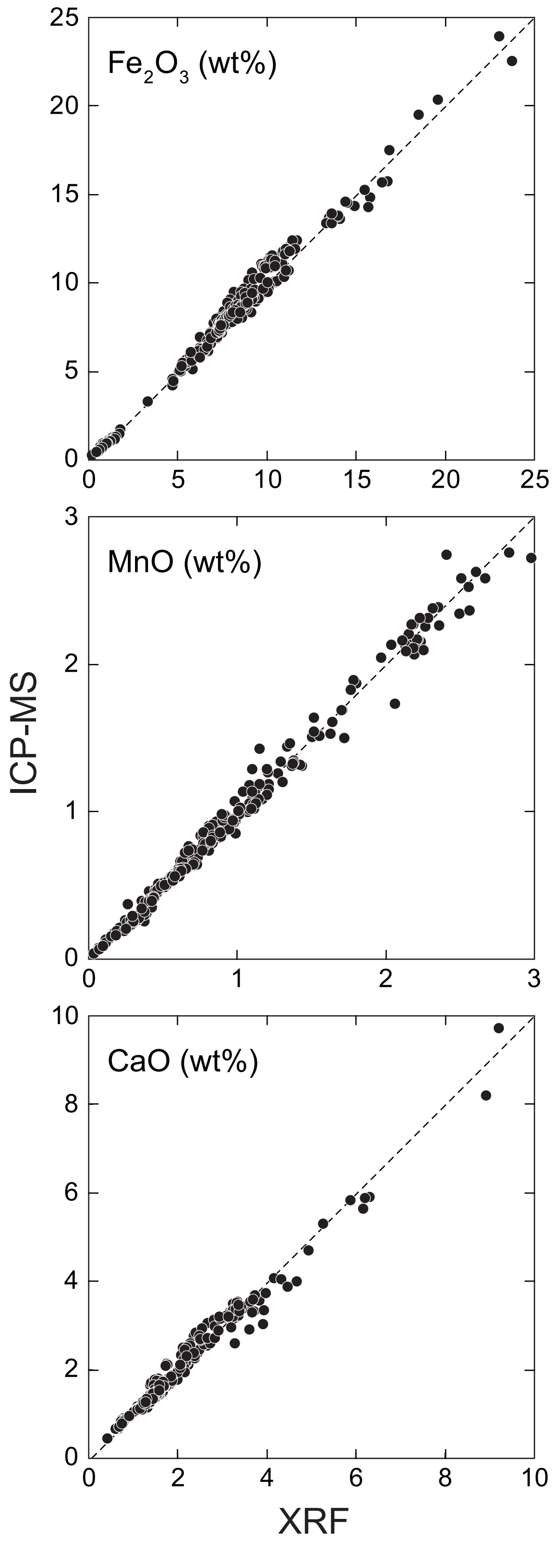

Supplementary Figure S10. Comparison of major element data obtained by two analytical methods (XRF and ICP-MS) for the piston core samples.

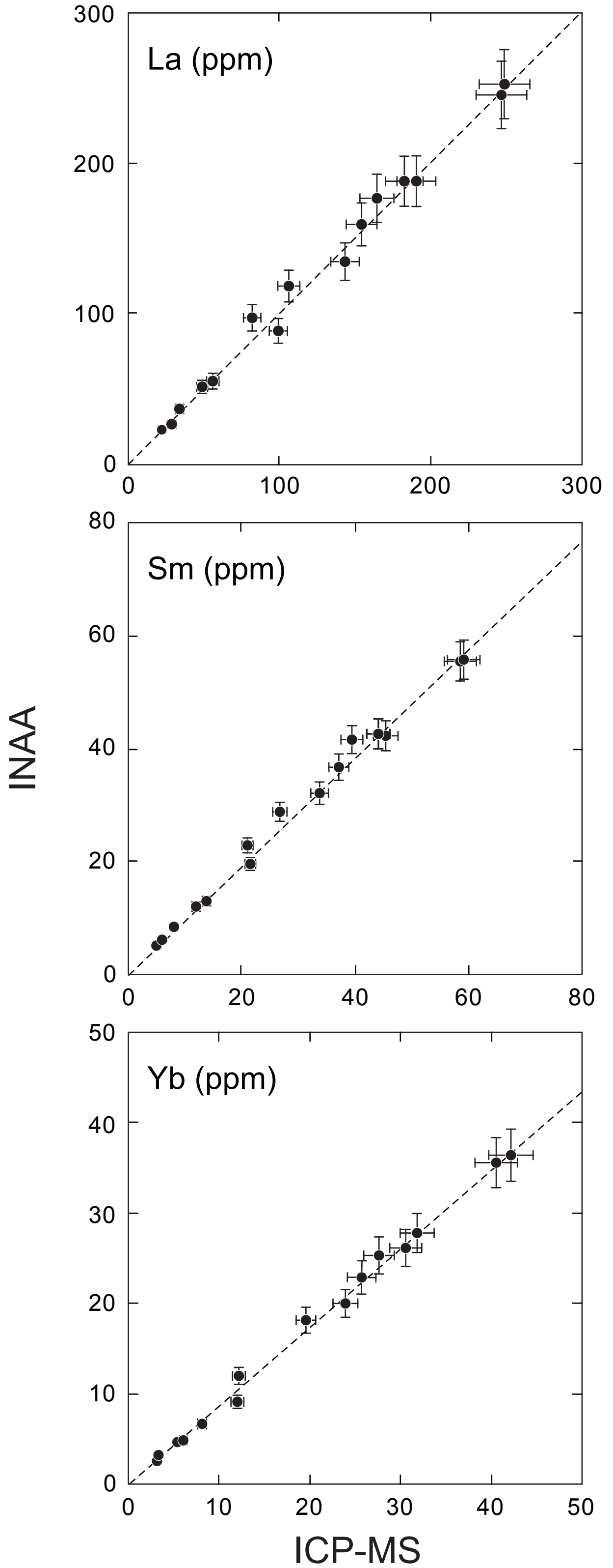

Supplementary Figure S11. Comparison of La, Sm and Yb data of selected core samples from Site 76 determined by the present ICP-MS analysis with INAA performed by Actlabs (Ontario, Canada). Error bars and dashed lines represent analytical uncertainties and regression lines, respectively. Our data agree well with the Actlabs data within the analytical uncertainties which integrate those for ICP-MS (<7 %) and INAA (<9 %), i.e., total <16 %. In these numerical values, uncertainties arising from 95 % confidence interval in the certified values of standard materials are included, and may produce a well-defined linear correlation with a systematic but minor deviation from the 1:1 trend (e.g., Yb). All the estimates concerning the potential storage in the main text are referred to considering the integrated uncertainties (e.g., ΣREY of 1,180 ± 189 ppm for Site 76).

Supplementary Table S1. DSDP/ODP and piston core lists used in this study.

(a) DSDP/ODP

Site	Hole	Latitude	Longitude	Water depth (m)	Area	Length of study core (m)
33	*	39°28.48'N	127°29.81'W	4,284	northeast Pacific	55.8
36	*	40°59.08'N	130°06.58'W	3,273	northeast Pacific	75.2
37	*	40°58.74'N	140°43.11'W	4,682	northeast Pacific	28.8
38	*	38°42.12'N	140°21.27'W	5,134	northeast Pacific	47.5
39	*	32°48.28'N	139°34.29'W	4,929	northeast Pacific	16.3
46	*	27°53'N	171°26.30'E	5,769	north central Pacific	6.35
65	*	04°21.21'N	176°59.16'E	6,130	central Pacific	73.0
68	*	16°43.32'N	164°10.36'W	5,467	central Pacific	16.4
71	*	04°28.28'N	140°18.91'W	4,419	central equatorial Pacific	68.5
74	*	06°14.20'S	136°05.80'W	4,431	southeast Pacific	36.3
75	*	12°31'S	134°16'W	4,181	southeast Pacific	79.5
76	*, A	14°05.90'S	145°39.64'W	4,598	southeast Pacific	27.1
83	*	04°02.80'N	95°44.25'W	3,646	eastern equatorial Pacific	18.4
160	*	11°42.27'N	130°52.81'W	4,940	central tropical Pacific	79.0
162	*	14°52.19'N	140°02.61'W	4,854	central tropical Pacific	36.0
163	*	11°14.66'N	150°17.52'W	5,230	central tropical Pacific	79.0
164	*	13°12.14'N	161°30.98'W	5,499	central Pacific	78.9
166	*	03°45.70'N	175°04.80'W	4,962	central Pacific	74.0
168	*	10°42.20'N	173°35.90'E	5,420	central Pacific	57.1
170	*	11°48'N	177°37'E	5,792	central Pacific	9.91
172	*	31°32.23'N	133°22.36'W	4,767	northeast Pacific	22.7
199	*	13°30.80'N	156°10.30'E	6,090	western Pacific	80.0
288	*	05°58.35'S	161°49.53'E	3,000	southwest Pacific	72.5
311	*	28°07.46'N	179°44.25'E	5,775	north central Pacific	20.4
313	*	20°10.52'N	170°57.15'W	3,484	central Pacific	78.5
316	*	00°05.44'N	157°07.71'W	4,451	central Pacific	8.81
317	B	11°00.09'S	162°15.78'W	2,598	central Pacific	70.0
319	*	13°01.04'S	101°31.46'W	4,296	southeast Pacific	55.8
463	*	21°21.01'N	174°40.07'E	2,525	north central Pacific	55.5
571	*	03°59.84'N	114°08.53'W	3,962	eastern equatorial Pacific	6.31
573	*, A	00°29.91'N	133°18.57'W	4,301	central equatorial Pacific	57.4
596	*	23°51.20'S	165°39.27'W	5,701	southwest Pacific	48.9
597	A	18°48.43'S	129°46.22'W	4,163	southeast Pacific	50.0
598	*	19°00.28'S	124°40.61'W	3,699	southeast Pacific	43.1
599	*	19°27.09'S	119°52.88'W	3,654	southeast Pacific	35.0
600	C	18°55.70'S	116°50.45'W	3,398	southeast Pacific	11.7
601	*	18°55.22'S	116°52.11'W	3,433	southeast Pacific	20.0
602	B	18°54.41'S	116°54.68'W	3,535	southeast Pacific	3.85
807	A	03°36.42'N	156°37.49'E	2,804	western equatorial Pacific	73.6
834	A	18°34.06'S	177°51.74'W	2,692	southwest Pacific	42.6
851	B	02°46.22'N	110°34.31'W	3,760	eastern equatorial Pacific	26.8
853	B	07°12.66'N	109°45.08'W	3,716	eastern equatorial Pacific	76.1
854	C	11°13.43'N	109°35.65'W	3,568	eastern equatorial Pacific	52.5
869	A	11°00.09'N	164°44.97'E	4,827	western Pacific	73.0
1215	A	26°01.77'N	147°55.99'W	5,396	central tropical Pacific	69.0
1216	A	21°27.16'N	139°28.79'W	5,153	central tropical Pacific	54.6
1217	A	16°52.01'N	138°06'W	5,342	central tropical Pacific	75.6
1218	A	08°53.37'N	135°22'W	4,826	central tropical Pacific	65.6
1220	A	10°10.60'N	142°45.49'W	5,218	central tropical Pacific	67.5
1221	A	12°02'N	143°41.65'W	5,175	central tropical Pacific	38.1
1222	A	13°48.98'N	143°53.35'W	4,989	central tropical Pacific	72.4

Supplementary Table S1. (*continued.*)

(b) Piston core

Cruise	Station No.	Latitude	Longitude	Water depth (m)	Area	Length of study core (m)
KH68-4	15-3	12°00'N	169°58.5'W	5,050	central Pacific	9.88
KH68-4	18-3	01°59.5'N	170°00.5'W	5,470	central Pacific	9.03
KH68-4	20-2	02°28.4'S	169°59.7'W	5,130	central Pacific	9.90
KH68-4	25-2	19°59.1'S	170°01.6'W	5,300	southwest Pacific	7.15
KH68-4	29-2	25°54.4'S	170°19.5'W	5,600	southwest Pacific	9.17
KH68-4	31-3	32°09.2'S	169°56.3'W	5,650	southwest Pacific	7.03
KH68-4	39-2	50°07.2'S	169°58.9'W	5,190	southwest Pacific	4.93
KH70-2	5-3	38°25.5'N	170°05.7'W	5,245	north central Pacific	10.6
KH70-2	7-3	33°01.9'N	169°53.5'W	5,420	north central Pacific	11.5
KH70-2	9-3	17°05'N	146°12.3'W	4,950	central tropical Pacific	4.19
KH71-5	7-2	02°00.8'N	145°59'W	4,550	central equatorial Pacific	10.0
KH71-5	10-2	04°58.5'S	146°03.5'W	4,960	southeast Pacific	2.02
KH71-5	12-3	11°01.4'S	146°01.5'W	4,830	southeast Pacific	2.95
KH71-5	15-2	20°23'S	148°02'W	4,615	southeast Pacific	0.72
KH71-5	42-2	27°34.8'S	88°03'W	3,690	southeast Pacific	4.60
KH71-5	44	21°S	93°W	−	southeast Pacific	3.87
KH71-5	53-2	08°15.3'N	112°42.1'W	3,380	eastern equatorial Pacific	5.27
KH72-2	56	21°34'N	132°42'E	5,360	Philippine Sea	7.50
KH72-2	58	22°53'N	129°13'E	5,300	Philippine Sea	7.51
KH73-4	5	12°23.2'N	151°48'E	5,920	western Pacific	11.5
KH73-4	9	07°49.9'S	172°48.6'E	5,390	central Pacific	10.3
KH76-2	3	24°27.2'N	132°35.4'E	4,750	Philippine Sea	6.97
KH80-3	22	31°16.2'N	153°42.9'E	5,750	western Pacific	10.5
KH80-3	30	09°50.6'N	153°13.5'E	5,480	western Pacific	10.0
KH84-1	17A	20°05.1'N	143°35'E	4,140	Philippine Sea	9.51
KH84-1	21	27°55.1'N	142°22.3'E	3,500	Philippine Sea	9.01
KH84-1	30	27°13.3'N	149°06.7'E	5,800	western Pacific	7.01

Supplementary Table S2. Total thickness and average ΣREY content of REY-rich mud in the two high-potential regions.

(a) the eastern South Pacific region

Site	Water depth (m)	Total thickness of REY-rich mud (m)	Average ΣREY content (ppm)
74	4,431	18.5	880
75	4,181	2.3	1,526
76	4,598	9.6	1,178
597	4,163	1.6	1,628
average	4,343	8.0	1,054*
range	4,163–4,598	1.6–18.5	880–1,628

(b) the central North Pacific region

Site	Water depth (m)	Total thickness of REY-rich mud (m)	Average ΣREY content (ppm)
65	6,130	16.8	451
68	5,467	16.4	886
160	4,940	17.4	488
162	4,854	4.4	495
163	5,230	23.4	660
164	5,499	29.8	720
166	4,962	8.6	506
168	5,420	7.1	680
170	5,792	9.9	1,002
313	3,484	5.7	727
1215	5,396	25.6	759
1216	5,153	43.7	603
1217	5,342	43.6	525
1218	4,826	37.8	569
1220	5,218	33.8	570
1221	5,175	6.4	472
1222	4,989	70.3	641
average	5,169	23.6	625*
range	3,484–6,130	4.4–70.3	451–1,002

* Note that the average ΣREY contents of the two high-potential regions are weighted averages.

Supplementary References

S1. Dubinin, A. V. Geochemistry of rare earth elements in oceanic phillipsites. *Lithology Mineral Res.* **35**, 101-108 (2000).

S2. Sheppard, R. A., Gude, A. J., III & Griffin, J. J. Chemical composition and physical properties of phillipsite from the Pacific and Indian Oceans. *Am. Mineral.* **55**, 2053-2062 (1970).

S3. Piper, D. Z. Rare earth elements in ferromanganese nodules and other marine phases. *Geochim. Cosmochim. Acta* **38**, 1007-1022 (1974).

S4. Taylor, S. R. & McLennan, S. M. *The Continental Crust: Its Composition and Evolution* (Blackwell, 1985).

S5. Gromet, L. P., Dymek, R. F., Haskin, L. A. & Korotev, R. L. The "North American shale composite": Its compilation, major and trace element characteristics. *Geochim. Cosmochim. Acta* **48**, 2469-2482 (1984).

S6. Goldstein, S. J. & Jacobsen, S. B. Rare earth elements in river waters. *Earth Planet. Sci. Lett.* **89**, 35-47 (1988).

S7. Floyd, P. A. & Castillo, P. R. Geochemistry and petrogenesis of Jurassic ocean crust basalts, Site 801. *Proc. ODP Sci. Results* Vol. 129, 361-388 (Ocean Drilling Program, 1992)

S8. Christie, D. M., Dieu, J. J. & Gee, J. S. Petrologic studies of basement lavas from northwest Pacific guyots. *Proc. ODP Sci. Results* Vol. 144, 495-512 (Ocean Drilling Program, 1995)

S9. Lécuyer, C., Reynard, B. & Grandjean, P. Rare earth element evolution of Phanerozoic seawater recorded in biogenic apatites. *Chem. Geol.* **204**, 63-102 (2004).

S10. Jarvis, I. Geochemistry and origin of Eocene-Oligocene metalliferous sediments from the central equatorial Pacific: Deep Sea Drilling Project sites 573 and 574. *DSDP Init. Repts.* Vol. 85, 781-804 (US Government Printing Office, 1985).

S11. Barrett, T. J., Taylor, P. N. & Lugowski, J. Metalliferous sediments from DSDP Leg 92: The East Pacific Rise transect. *Geochim. Cosmochim. Acta* **51**, 2241-2253 (1987).

S12. Barrett, T. J. & Jarvis, I. Rare-earth element geochemistry of metalliferous sediments from DSDP Leg 92: The East Pacific Rise transect. *Chem. Geol.* **67**, 243-259 (1988).

S13. Iwamori, H., Albarède, F. & Nakamura, H. Global structure of mantle isotopic heterogeneity and its implications for mantle differentiation and convection. *Earth Planet. Sci. Lett.* **299**, 339-351 (2010).